

PROJECT ADMINISTRATION DATA SHEET

ORIGINAL REVISION NO. _____

Project No. G-33-A11 05250-1A0 ~~GTRG/GIT~~ DATE 5 / 16 / 86

Project Director: Dr. Nai-Teng Yu School/~~ES~~ Chemistry

Sponsor: DHHS/PHS/NIH/NEI

Type Agreement: Grant No. 5 R01 EY01746-11

Award Period: From 5/1/86 To 4/30/87 (Performance) 4/30/87 (Reports)

Sponsor Amount:	<u>This Change</u>	<u>Total to Date</u>
Estimated: \$	<u>112,039</u>	\$ <u>112,039</u>
Funded: \$	<u>112,039</u>	\$ <u>112,039</u>

Cost Sharing Amount: \$ 5,830 Cost Sharing No: G-33-322 (E5250-1A0)

Title: Comparative Raman Studies of Human and Animal Lenses

ADMINISTRATIVE DATA

1) Sponsor Technical Contact:	OCA Contact <u>E. Faith Gleason X-4820</u>	2) Sponsor Admin/Contractual Matters:
<u>Henry N. Fukui, PhD</u>	<u>Donna D. Adderly</u>	
<u>Extramural Program Director</u>	<u>Grants Management Section</u>	
<u>Contract Division</u>	<u>Extramural Services Branch</u>	
<u>National Eye Institute</u>	<u>National Eye Institute</u>	
<u>Bethesda, Maryland 20892</u>	<u>Bethesda, Maryland 30892</u>	
	<u>(301) 496-5884</u>	

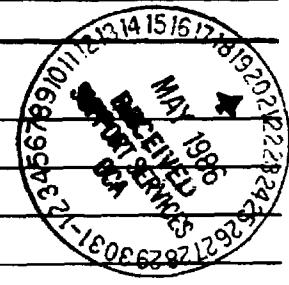
Defense Priority Rating: N/A Military Security Classification: N/A
(or) Company/Industrial Proprietary: _____

RESTRICTIONS

See Attached NIH Supplemental Information Sheet for Additional Requirements.
Travel: Foreign travel must have prior approval - Contact OCA in each case. Domestic travel requires sponsor approval where total will exceed greater of \$500 or 125% of approved proposal budget category.
Equipment: Title vests with GIT

COMMENTS:

Continuation of G-33-A10



COPIES TO: SPONSOR'S I. D. NO. 02,108,001,86,018

Project Director	Procurement/EES Supply Services	GTRC
Research Administrative Network	Research Security Services	Library
Research Property Management	Reports Coordinator (OCA)	Project File
Accounting	Research Communications (2)	Other <u>Jones; Legal</u>

SPONSORED PROJECT TERMINATION/CLOSEOUT SHEET

N-2
AK12

Date 6-4-87

Project No. G-33-A11

School XXX Chemistry

Includes Subproject No.(s) N/A

Project Director(s) Dr. Nai-Teng Yu

GTRC / GIT

Sponsor DHHS/PBS/NIH/NEI

Title Comparative Raman Studies of Human and Animal Lenses

Effective Completion Date: 4/30/87 (Performance) 4/30/87 (Reports)

Grant/Contract Closeout Actions Remaining:

- None
- Final Invoice or Final Fiscal Report
- Closing Documents
- Final Report of Inventions
- Govt. Property Inventory & Related Certificate
- Classified Material Certificate
- Other _____

Continues Project No. G-33-A10

Continued by Project No. G-33-A12

COPIES TO:

Project Director
 Research Administrative Network
 Research Property Management
 Accounting
 Procurement/GTRI Supply Services
 Research Security Services
 Reports Coordinator (OCA)
 Legal Services X

Library
 GTRC
~~RESEARCH ADMINISTRATION~~
 Project File
 Other Duane H.
Angela DuBose
Russ Embry

MICROBEAM RAMAN/FLUORESCENCE ANALYSIS OF EYE LENS

Nai-Teng Yu, Ming-Zhi Cai, Deborah J.-Y. Ho, Fred L. Thompson
and John F. R. Kuck

We report the design and performance of a new automated laser micro-Raman/fluorescence spectroscopic scanning system for obtaining two-dimensional concentration profiles of protein constituents and various cataract-related fluorophors in the eye lens. Our microprobe system is capable of (1) automated acquisition of "position-defined" Raman/fluorescence spectra from gridded points (1-2 μm diameter) of a lens section, (2) storage of intensity data of up to six spectral lines (or integrated fluorescence intensity) from each point, (3) six-color graphic 3-D topographic presentation of gridded data set, and (4) plotting of contours intersecting the intensity data with constant height planes. The instrumentation consists of (1) a modified Zeiss microscope with a video camera and two computer-controlled actuators, (2) a modified Spex 1877 Triplemate, (3) a multichannel detector (PAR model 1420 Intensified Reticon) and (4) an IBM XT computer with home-built interface boards for controlling the detector, a programmed electronic shutter and the X-Y stage translator. Available lasers are He-Cd, Ar⁺, Kr⁺ and N₂. This system is expected to be useful for obtaining relevant information pertaining to the modes of fluorophor production and the mechanisms of cataract formation. The method is applicable to any lenses (human/animal; normal/cataractous).

Authors Yu, Cai, Ho and Thompson are at Georgia Institute of Technology (Department of Chemistry), Atlanta, Georgia 30332; author Kuck is at Emory University (Department of Ophthalmology), Atlanta, Georgia 30332. National Eye Institute supports (EY01746 and EY00260) are acknowledged.

Experimental

Human lenses were obtained from the Atlanta Lions Eye Bank. Before preparation of a flat lens surface for X-Y data collection, the lens was frozen (at -80°C) in an aluminum rectangular trough whose depth and width are equal to the equatorial radius and optical axis length, respectively. The lens was so positioned that its optical axis is horizontal and one-half of the lens was above the top-surface of the aluminum block. The entire aluminum block with a frozen lens in its trough was then transferred to the thermoelectric cold plate (-50°C) affixed to the X-Y translation stage. After the upper half of the lens was shaved away by a knife, the lower half with a flat surface was then covered by a layer of glycerol and a thin microscopic slide. Dry nitrogen gas was then channeled into the surrounding of the frozen lens surface via a circular glass apparatus which enclosed the cold plate and the aluminum block, but still allows the microscope objective lens to approach the sample surface.

A typical laser scanning path on the lens section is shown in Fig. 1. The scanning domain is $\sim 11\text{ mm} \times 6\text{ mm}$, which is somewhat larger than the rectangular trough. A total of 600 data points (20×30) from a lens section were routinely obtained. To obtain a better resolution, a total of 2,000 data points (40×50) was obtained. The anterior side has a less curvature than the posterior side.

Results and Discussion

We report here the testing of the performance of our automated laser microprobe scanning system, using a 22-year old human lens. It is well-known that the human lens contains numerous fluorophors depending on age and pathological state.¹ In the present study, we monitored the fluorophor which

exhibits an emission maximum at ~ 525 nm when excited at 441.6 nm (He-Cd laser). The spatial distribution of this fluorophor on the lens section is shown in Fig. 2. It is interesting to note that near the optical axis there is a higher concentration of fluorophor toward the anterior side (see Fig. 2c). On the other hand, there is an apparent minimum near the center when one views the graph along the optical axis (see Fig. 2d). Detailed interpretation of the topographic contour (Fig. 2a) and the profiles in Fig. 2(c) and 2(d) must await the studies of profiles using integrated fluorescence intensities, instead of the peak intensity at 525 nm. The problem involves the conversion of one fluorophor to a different fluorophor during aging, resulting in a shift in emission maximum to a longer wavelength.

Studies of fluorophors distributions in the eye lens are important because of the popular belief that these fluorophors are generated by photocatalyzed reactions which may be the initiating event for the formation of nuclear senile cataract.²⁻⁴ The hypothesis that the lens may be affected adversely by the radiation which it absorbs is a reasonable one, although evidence in favor of such a relationship is only circumstantial. Studies of the epidemiology of this type of cataract always cite the elevated incidence in Tibet (China), India and Pakistan as perhaps being due primarily to the high intensity of light reaching the eye in a tropical population. Retrospective studies on human cataract offer little hope of proving the hypothesis and results of experimental studies on animals subject to near ultraviolet (UV) radiation are difficult to correlate with human cataracts for lack of suitable models.

If human nuclear cataract (brunescent type) is caused by light, the pigment or fluorophor accumulation should have certain geometrical characteristic which follow because of this mode of production. First, since

near UV light strikes the anterior part of the nucleus first and is absorbed there in all but very young lenses, the pigmented zone should expand anteriorly but not posteriorly. The shape of the pigmented nucleus in an older person should then be asymmetrical along the optical (visual) axis. Secondly, because of the action of the pupillary system in regulating the light allowed to enter the eye, the more intense the light, the more the beam is restricted to a pathway coincident with the optical axis. Thus, viewed at the anterior pole along the optical axis the pigmented zone should be darker at the center. Such an effect is not noticeable because it is indistinguishable from the apparent greater central absorption due entirely to the fact that the optical axis passes through the thickest part of the lens which interposes more pigment in the light path. Thirdly, since the outer anterior zone of the nucleus protects the inner anterior zone from the effect of the light, pigment concentration should exhibit little increase as one goes toward the center of the nucleus.

These conclusions, arrived at intuitively, can hardly be verified by observing the whole lens in vitro. The proof may come from determinations of the detailed spatial distribution of various fluorophors. Our automated Raman/fluorescence microprobe topographic system is designed for routine analysis of fluorophor and lens constituents distributions on the surface of a dissected lens. By analyzing a large number of human lenses of all ages (both normal and cataractous) and different sources (in particular those from Tibet), we should be able to draw conclusions about the mode of production of each fluorophor in human lens.

References

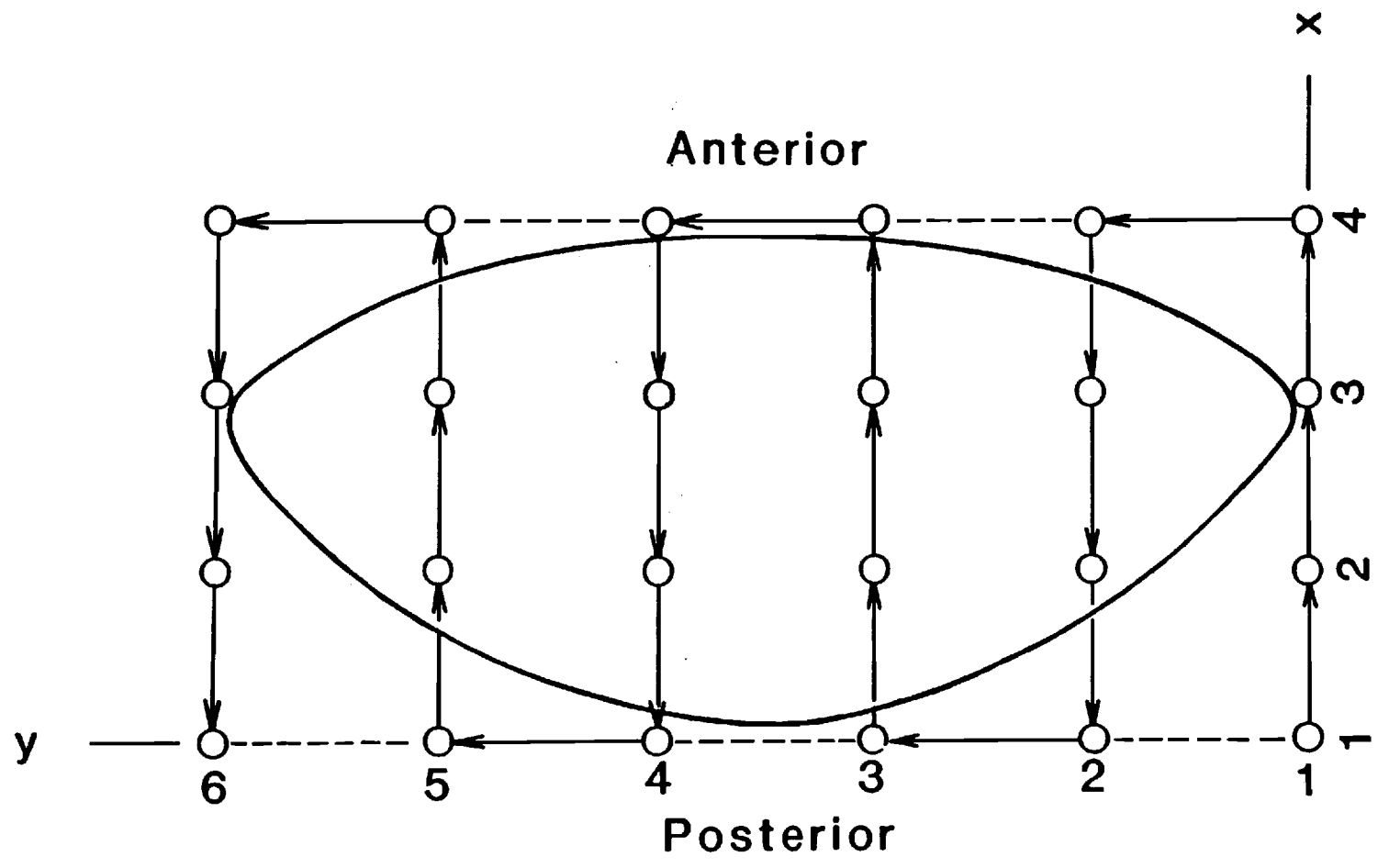
1. N.-T. Yu, M. Bando and J. F. R. Kuck, Invest. Ophthalmol. Vis. Sci. 26, 97-101 (1985).
2. A. Pirie, Invest. Ophthalmol. 7, 634-50 (1968).
3. R. F. Borkman, A. Dalrymple and S. Lerman, Photochem. Photobiol. 26, 129-132 (1977).
4. R. C. Augusteyn, Jpn. J. Ophthalmol. 18, 127-34 (1974).

Figure Captions

Fig. 1 The ocular lens section confined in a 11 mm x 6 mm rectangular domain for two-dimensional grid data collection. Raman/fluorescence signals are obtained from 600-2,000 points ($\sim 2 \mu\text{m}$ diameter). The laser scanning path is indicated with arrows.

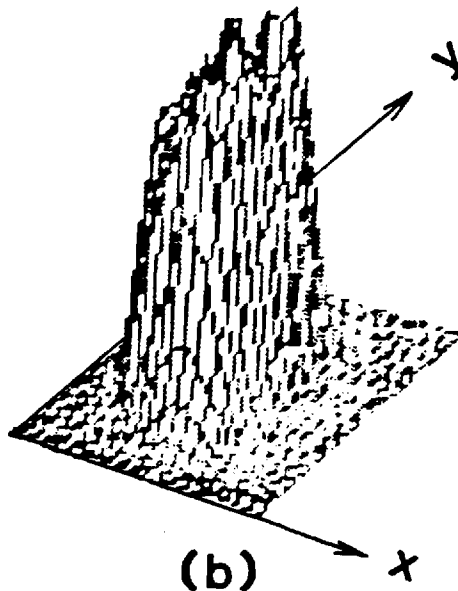
Fig. 2 Fluorophor distribution in a 22-year old human lens. The lens section was made along the optical axis and perpendicular to the equatorial plane. The fluorophor exhibits an emission maximum at 525 nm when excited at 441.6 nm. The peak intensity at 525 nm has been used to obtain the distribution profiles. (a) topographic contour map: the lowest contour level, 645 counts; the maximum intensity, 3683 counts; the contour interval step value, 217; (b) 3-D graphic presentation of X, Y data set; (c) a view of plot (b) along y-axis (tilt angle = 0; spin angle = 0); (d) a view of plot (b) along x-axis (tilted angle = 28°; spin angle = 90°).

Fig. 1
Yu, Cai, Ho,
Thompson and Kuhl

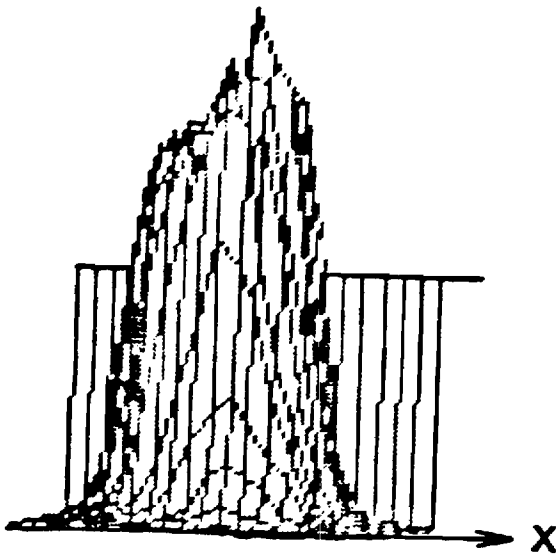




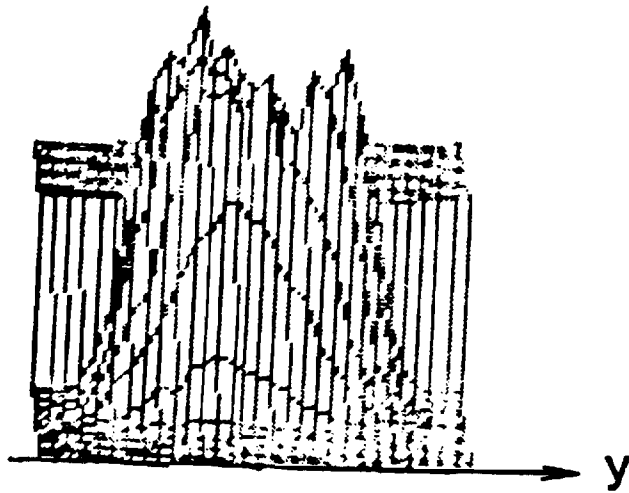
(a)



(b)



(c)



(d)

Raman Spectroscopic Evaluation of Aging and Long-wave UV Exposure in the Guinea Pig Lens: A Possible Model for Human Aging.†

† This work was supported by the National Eye Institute grants EY01746 (NTY) and EY00260 (JFRK). The Emory University Department of Ophthalmology has a grant from Research to Prevent Blindness.

Brent C. Barron†§, Nai-Teng Yu†§*, John F. R. Kuck, Jr.§

School of Chemistry, Georgia Institute of Technology, Atlanta, Georgia 30332 and Department of Ophthalmology, Emory University School of Medicine, Atlanta, Georgia 30322.

Running title: Disulfide & Sulfhydryl in the Guinea Pig Lens

Key words: Raman, Lens, Disulfide, Sulfhydryl, Aging, UV

† Georgia Institute of Technology
§ Emory University

*address correspondence to this author

The laser Raman optical dissection technique makes it possible to study individual points of minute volumes (2×10^{-3} ul) in the intact living lens, in vitro. This technique was used to measure the sulfhydryl and disulfide content of 21 distinct points along the visual axis of the guinea pig lens after aging and long-wave ultraviolet exposure (9 month duration, in vivo). To facilitate comparison between different lenses, data was compiled as the intensity ratio of sulfhydryl (2580 cm^{-1}) to a protein reference signal (2731 cm^{-1}) or disulfide (508 cm^{-1}) to phenylalanine (622 cm^{-1}). These 21 ratios for each experiment were plotted as a function of the distance of the point from the geometric nuclear center of the lens to give a visual axis profile. From these profiles we have found that the loss of sulfhydryl can be accelerated in the guinea pig lens by in vivo ultraviolet exposure (353 nm peak from an incoherent source) for 9 months. There is also a subsequent uniform increase in the disulfide content across the visual axis suggesting a direct sulfhydryl to disulfide conversion in the guinea pig lens.

Introduction

Maintainence of ocular lens transparency is essential for proper visual functioning. Any changes in the lens (traumatic metabolic, or pathologic) which preceed and/or contribute to lens opacification (cataract) need to be studied and defined so that these processes can be understood. Raman spectroscopy can be used as a noninvasive probe in lens research to monitor many structural and biochemical changes in the intact lens during normal aging or after ultraviolet (UV) irradiation.

A biochemical change which has been implicated as an aging effect is the conversion of free sulfhydryl (SH) to disulfide (S-S) which may be a mechanism involved in senile cataract formation in some mammals (East et al., 1978; Askren et al., 1979; Kuck et al., 1982; Ozaki et al., 1983; Itoh et al., 1983; Yu et al., 1985). Whether S-S formation is a causitive or stabilizing factor in nuclear and senile cataractogenesis is still under debate. Lens brunescence and nuclear cataractogenesis have been correlated to increasing oxidation of sulfhydryl compounds in the human lens (van Haard et al., 1980), however, this conclusion was determined from lens homogenates and may be partially artifactual due to the exposure of the homogenates to air. A more recent study (Yu et al., 1985) shows that there is a 50% loss in SH in the intact human and guinea pig lens during aging but there is no accumulation of disulfide over the lifespan of the subject. In these cases, it is believed glutathione (GSH) maintains reduced protein SH (PSH) by

reacting with protein disulfides (PS-SP) to yield a mixed glutathione-protein disulfide (GS-SP) and PSH. The GS-SP is then reduced by glutathione reductase to yield another PSH and oxidized glutathione (GS-SG) which is subsequently extruded from the lens. This conclusion explains the loss of SH with no detectable increase in SH oxidation products. It was also shown that SH to S-S conversion in intact rat and mouse lens is not necessarily related to nuclear senile cataract formation but is a normal aging phenomenon since old lenses with extensive SH oxidation and S-S accumulation remained clear. This particular study used the Raman optical dissection technique which offers an advantage in ocular lens research. The lens remains intact and the proteins in situ in a low oxygen environment, insuring no artifactual oxidation of sulfhydryl, an inherent problem in studying lens homogenates. The technique allows the measurement of the Raman signals from sulfhydryl S-H stretching vibration (2580 cm^{-1}) and disulfide (508 cm^{-1}) from very specific points of minute volumes ($2 \times 10^{-3}\text{ ul}$) in any desired area of the lens. When the intensities of the sulfhydryl and disulfide signals are standardized by the intensities of a protein reference (2731 cm^{-1}) (the absolute intensity is a measure of protein concentration [Askren et al., 1979]) or phenylalanine (622 cm^{-1}) signals, respectively, a visual axis profile can be constructed and compared for each lens studied. A visual axis (VA) profile is a two dimensional representation of the lens VA with respect to one of its measureable components (i.e. sulfhydryl, disulfide, aromatic amino acids, fluorescence, etc.). Each data point in the profile is determined by an intensity ratio

from one spectrum taken from a specific point along the VA. The VA profile of each lens can be used as a basis for comparison between lens of varying age and between normal and UV irradiated lenses.

Comparing the sulfhydryl and disulfide profiles from different lenses would reveal if any loss in SH is concurrent with an increase in S-S during aging or UV irradiation. In the mouse and rat lens, there is a precipitous fall in the amount of free SH in the nucleus during aging with an increase in the S-S in this region (Askren et al., 1979). This extensive sulfhydryl oxidation in the rat and mouse lens is a normal aging phenomenon, however, as discussed above the human and guinea pig lens do not exhibit this age-dependent change in nuclear S-S or SH. These results suggest that the guinea pig lens may be a good model for human aging since under normal conditions they are very similar. It is of interest then to extend these studies to the effects of long-wave UV on the SH content of the guinea pig lens.

In this study we present evidence that the loss of SH can be accelerated by in vivo long-wave UV exposure in the guinea pig lens, with a subsequent increase in the disulfide content. The decrease of sulfhydryl in the normal aging guinea pig lens is not concomitant with an increase in disulfide suggesting that long-wave UV may be responsible for a direct $2 \text{ SH} \rightarrow \text{S-S}$ conversion .

Experimental Procedures

Materials

Guinea pigs were maintained under standard conditions. Housing conditions for normal aging and UV irradiated guinea pigs have been previously described (Barron et al., in press) Enucleated guinea pig eyes were immediately dissected and the lens placed in a nutritive media containing 0.9% saline, phosphate buffer, and glucose. All experiments were begun within one hour after enucleation. In vivo irradiation was accomplished using a General Electric UV lamp (F-15T8) which has a 300-400 spectral distribution with a maximum intensity at 353 nm. Animals were exposed to 1.3 mW/cm^2 continually for 9 months from time of weaning.

Methods

The lens was placed anterior down in a cuvette containing the nutritive media which was then mounted on a precision translation stage. A laser beam was directed from below and focused along the visual axis. The image of the laser passing through the sample was focused on the entrance slit of a Spex 1401 double monochromator. The length of the VA was equally divided into 21 successive points; a spectrum from each point was obtained by analyzing the Raman scattered light 90° from the incident laser beam using a laser Raman spectrometer. A complete description of the Raman optical dissection technique has been described previously (Askren et al., 1979). The present system consisted of a RCA type C-31034

photomultiplier tube and a Spex DM1B Spectroscopy Laboratory Coordinator. Obtained spectra was smoothed by an 11 point algorithm (Savitsky and Golay, 1964) to improve the signal to noise ratio and plotted on a Houston Instruments DMP-40 digital plotter. A Coherent Radiation model CR-5 argon-ion laser provided an excitation wavelength of 514.5 nm. The beam was passed through a laser mate to remove plasma lines and through a series of optical filters so that the final power at the sample was 200-250 milliwatts. The sulfhydryl region was scanned from 2500 to 2850 cm^{-1} and the disulfide region from 450 to 700 cm^{-1} . Each point along the VA was scanned 5 times using a repscan program for the Spex DM1B. Scan parameters were set as follows: 1.0 cm^{-1} increments with an integration time of 0.5 seconds per increment, slit width 300 μ , slit height 2 mm.

Disulfide profiles were constructed by standardizing the intensity of the disulfide signal at 508 cm^{-1} by the phenylalanine signal at 622 cm^{-1} for each of the 21 spectra taken along the VA. The intensity ratio was plotted against the distance the point was from the geometric nuclear center of the lens. Each ratio represents a different point along the VA corresponding to a scattering volume of 2×10^{-3} μl . Sulfhydryl profiles were constructed similarly using the intensity ratio of sulfhydryl (2580 cm^{-1}) to the protein reference signal (2731 cm^{-1}). Curves for the VA profiles were generated from data points using a least squares fit to a third order equation.

Results

A typical Raman spectrum of the guinea pig lens is shown in Figure 1. This spectrum was taken from the geometric nuclear center of a 9 month old normal lens. Strong amide I and III signals at 1670 and 1240 cm^{-1} , respectively, indicate the proteins are in an anti-parallel β -pleated sheet conformation (Yu et al., 1974; Lord and Chen, 1974). Changes in the intensities of these signals would reveal if there is a protein conformational change (to random coils or α -helical), however, no change could be detected after UV irradiation or during aging. Other important signals originate from tyrosine (644 cm^{-1}), tryptophan (760 cm^{-1}), aromatic fingerprint region (830, 855, and 880 cm^{-1}), phenylalanine (1006 cm^{-1}), and CH_2 deformation (1450 cm^{-1}). The regions for disulfide (450-700 cm^{-1}) and sulfhydryl (2450-2850 cm^{-1}) are expanded in Figure 2 to show how intensities were measured to obtain the ratios used in VA profile construction. These spectra are from the same 9 month old normal lens. Each of the 21 spectra were analyzed similarly and the ratios I_{508}/I_{622} and I_{2580}/I_{2731} were used as data points in the profile. The phenylalanine signal was used as an internal standard for disulfide since in the guinea pig lens, the concentration of phenylalanine is linear with respect to protein along the VA from anterior to posterior poles. This result was determined by phenylalanine to amide I ratios (I_{622}/I_{1670}) and is shown in Figure 3. Amide I is considered to be an indicator of protein concentration. Similarly, 2731 cm^{-1} was used to standardize sulfhydryl since it is also a protein reference signal. These

standardized ratios represent relative concentrations of total sulfhydryl or disulfide per unit protein.

A comparison of VA profiles from normal lenses of different ages is shown in Figure 4. There is a gradual decrease in the amount of free sulfhydryl with approximately a 10% loss of in the nucleus of the 9 month old lens as compared to a 2 month old. There is a slightly greater loss of SH in both anterior and posterior cortices (12-15%). The increase in the length of the VA is due to normal growth of the lens. For the 9 month old lens, only 20 data points were analyzed. The signals of the outermost point on the anterior side of the lens were lost in the background noise. This problem is occasionally encountered and is due to an unusual amount of excessive scattering at the capsule interface. Once the lens has been exposed to long-wave UV light for 9 months (in vivo), there is an accelerated loss of SH present in the lens. Figure 5 shows that there is a greater loss of SH in the lens nucleus (up to 50%) where the oldest fibers are located, with only a 20% loss in the cortices after UV exposure.

To determine if a similar depression of SH could be reproduced in vitro, a lens was exposed to 325 nm irradiation from a He-Cd laser for 5 hours. The power at the sample was 9 mW/mm^2 (160 J/mm^2 total exposure). Figure 6 shows the result of this experiment. After in vitro UV exposure there is no decrease in the sulfhydryl content as compared to normal lens of the same age. The 2 VA profiles represent contralateral lenses; during the UV exposure, one

lens was analyzed by Raman. Afterwards the UV exposed lens was analyzed.

To determine if a loss of sulfhydryl correlated to an increase in the disulfide content of the lens after in vivo UV exposure, disulfide profiles from a 9 month old normal and 9 month old irradiated lens were compared (Figure 7). The same lenses used to collect data for the SH profiles in Figure 5 were used to obtain S-S data. The amount of disulfide in the normal lens is 50% less than that found in the UV exposed lens. The differences in the cortices are not as pronounced with only a 20-25% difference in accumulated disulfide.

Discussion

Studies have shown that the mouse and rat lens exhibit remarkably different behavior from the guinea pig and human lens with respect to disulfide and sulfhydryl patterns along the VA during normal aging (Yu et al., 1985). The mouse and rat show a precipitous fall in the amount of SH in the nuclear region of the lens with a concomitant rise in the S-S in this region. The guinea pig and human lens, however, show a gradual decline in SH with very little accumulation in S-S. These results indicate that the guinea pig may be a good model for the human lens. We have extended the normal aging studies to include the effect of UV on the total SH content of the guinea pig lens and to determine if there is a measurable increase in the amount of S-S during the exposure.

In the present study, we have demonstrated that the loss of SH can be accelerated in the guinea pig lens by in vivo long-wave UV exposure. Following a 9 month exposure there is a uniform increase in the S-S across the VA of the lens. After this exposure time the lens remains clear with no sign of visible nuclear opacities or pigmentation (the guinea pig lens does not accumulate visible pigments, a distinction between it and the human lens). This fact suggests that in the guinea pig lens disulfide bond formation is not cataractogenic, however, other studies show it is at least a stabilizing effect in mature cataracts. Anderson and Spector (1978) have shown that at least 90% of the water insoluble protein sulfhydryl groups are oxidized in mature human cataracts. These results have been confirmed by other groups (Anderson et al., 1979; Spector and Roy, 1978; Garner and Spector, 1980; Kuck and Kuck, 1983).

In our studies we have found an approximate 1.2 SH/unit protein in the nuclear region of a 9 month old normal guinea pig lens (Figure 5). After continuous long-wave UV irradiation for the 9 month period this value drops to 0.6 SH/unit protein, indicating a 50% reduction (0.6 SH/unit protein) in the total sulfhydryl present in a normal lens. Concomitantly, there is a 100% increase in the amount of S-S present in the same lens (Figure 6), going from 0.06 S-S/unit protein in the normal 9 month old lens to 0.12 S-S/unit protein in the irradiated lens. These results suggest that of the total SH lost (0.6 SH/unit protein) 20% is directly converted to S-S (0.12 SH/unit protein \rightarrow 0.06 S-S/unit protein) during in vivo UV

exposure. The fact that high power short term UV exposure (325 nm from a laser) does not effect the SH content of the lens (Figure 6) suggests that the remaining reduction in free sulfhydryl is probably due to long term processes such as aberrant protein synthesis, inactivation of the glutathione reductase pathway, or an accelerated depletion of the reduced glutathione pool (oxidized glutathione could be subsequently extruded from the lens). All these processes would effect the amount of SH in the lens without effecting the measured disulfide.

There is no change in the secondary structure after SH oxidation as indicated by the strong amide I signal at 1670 cm^{-1} (Figure 1) during aging or after UV irradiation. These results imply that the free sulfhydryls are clustered together in near proximity to each other in such a way that oxidation of SH to form intra- or inter-molecular S-S does not involve protein unfolding of the secondary structure. This observation is in agreement with previous studies on intact rat lenses (Yu and Kuck, 1981). There are possibly microenvironmental changes in the side chains of amino acid residues, particularly tryptophan, as well as tertiary structural changes (Yu and Kuck, 1981; Ozaki et al., 1983) after UV exposure, however these possibilities were not addressed in this study.

The use of the guinea pig lens as a human model is an important tool in studying long term effects of UV on the eye lens. Normal aging studies have shown the similarities between the lenses of

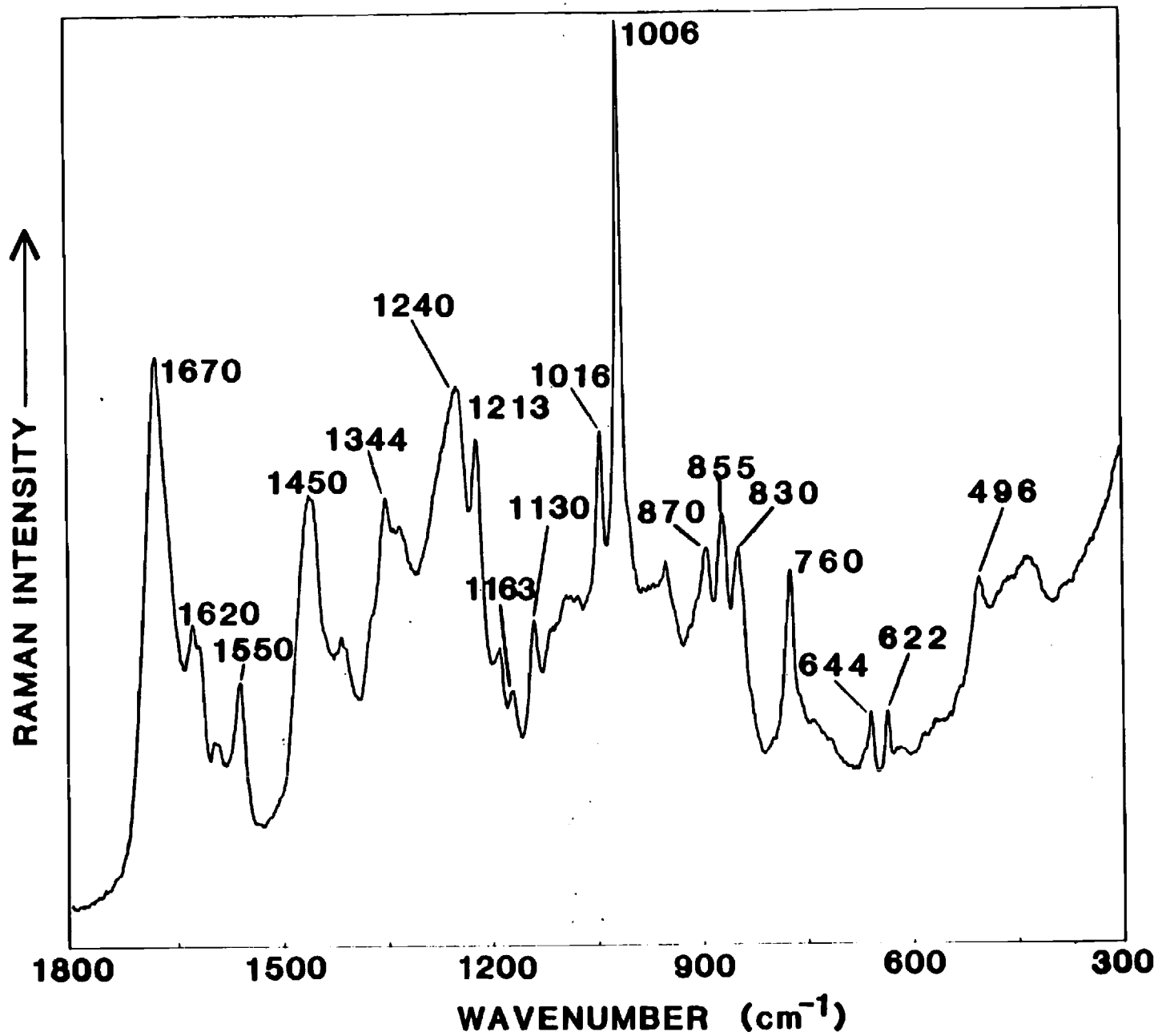
these two species, thus, the preceding studies on the guinea pig lens allow us to extend our understanding of aging and cataractogenic processes in the human lens. We have shown that the use of short term UV exposure has limited applications to aging processes and that a proper animal model is essential in studying long term effects on the lens to extend our knowledge of these processes.

References

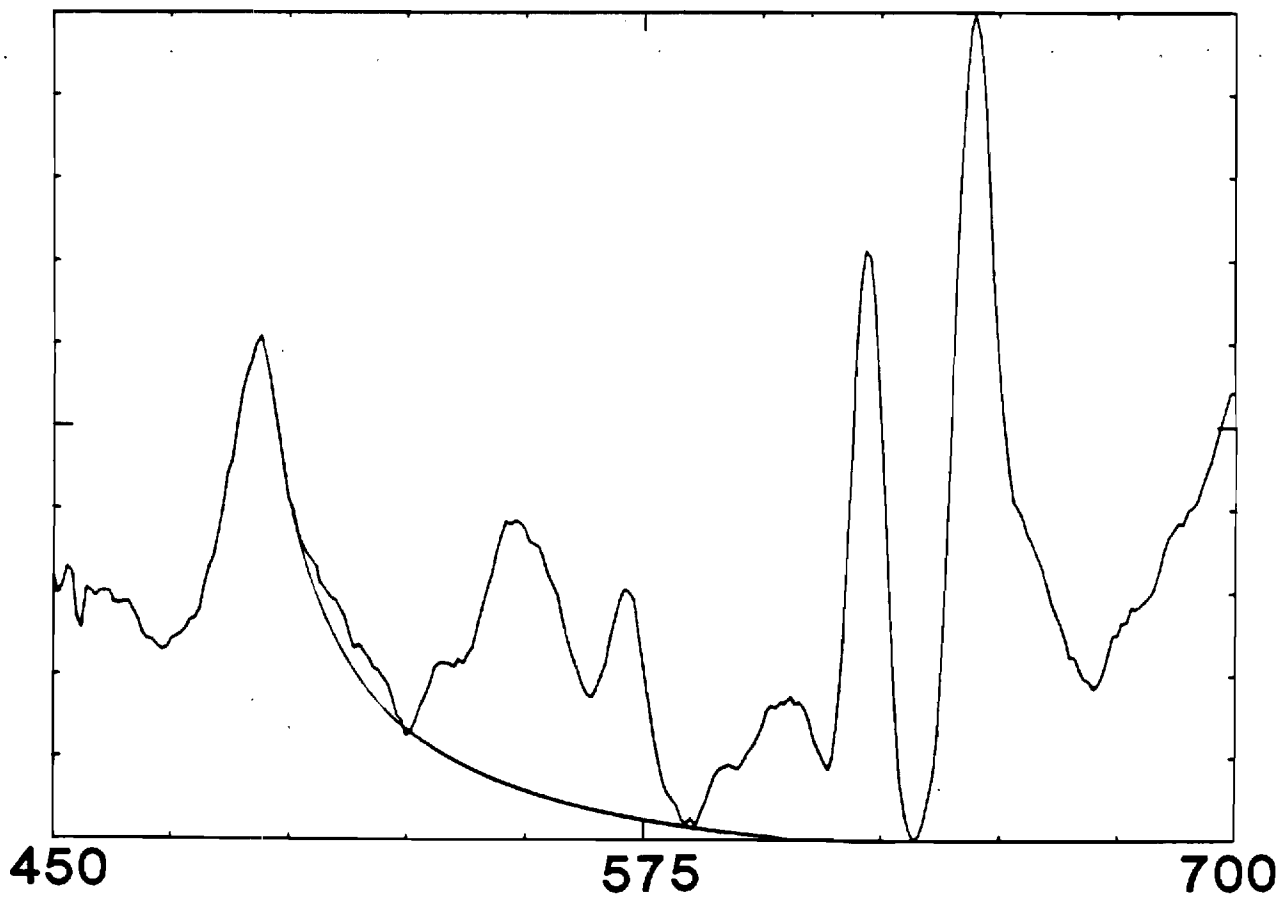
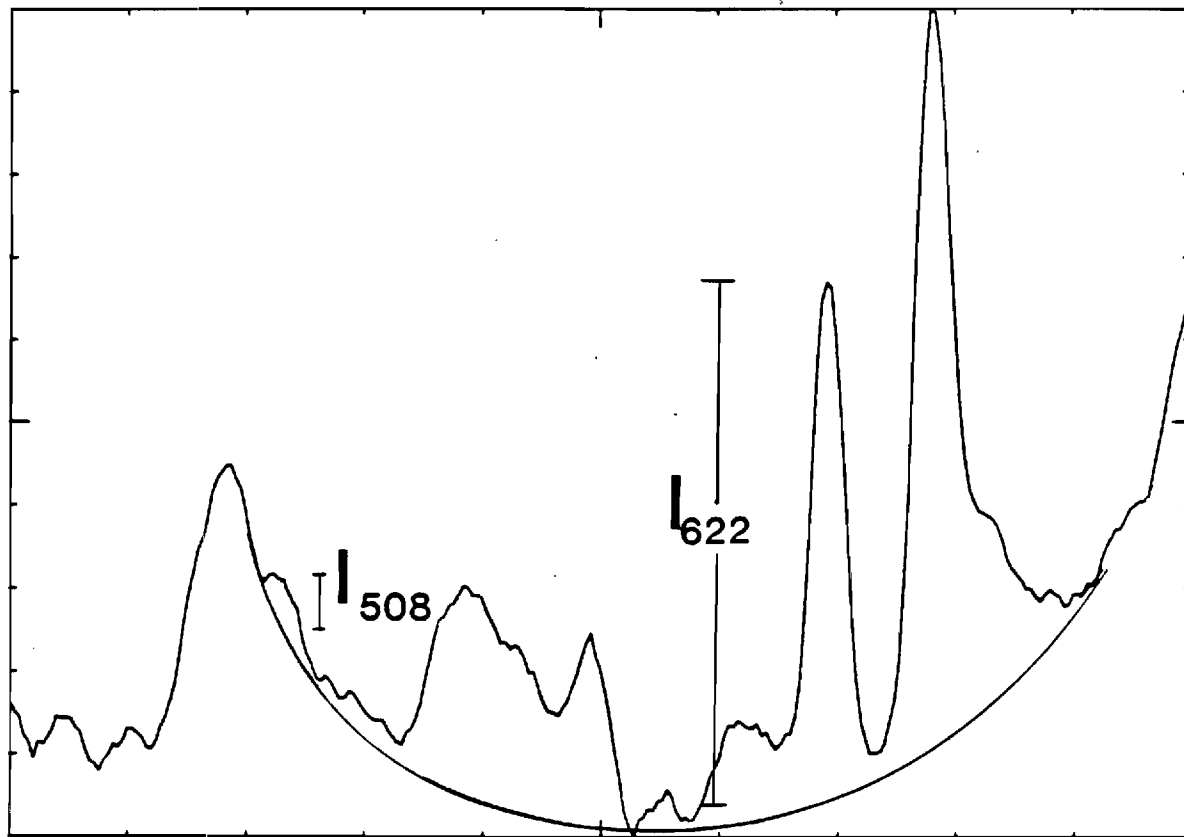
- Anderson, E.I. & Spector, A. (1978) *Exp. Eye Res.* 26:407-417.
- Anderson, E.I., Wright, D.D. & Spector, A. (1979) *Exp. Eye Res.* 29:233-243.
- Askren, C.C., Yu, N.-T., & Kuck, J.F.R. (1979) *Exp. Eye Res.* 29: 647-654.
- Barron, B.C., Yu, N.-T., & Kuck, J.F.R. (in press) *Invest. Ophthalmol. Vis. Sci.*
- Chen, M.C. & Lord, R.C. (1974) *J. Amer. Chem. Soc.* 96: 4750.
- East, E.J., Chang, R.C.C., Yu, N.-T., & Kuck, J.F.R. (1978) *J. Biol Chem.* 253:1436-1441.
- Garner, M.H. & Spector, A. (1980) *Proc. Natl. Acad. Sci.* 75:3244-3248.
- Itoh, K., Ozaki, Y., Mizuno, A., & Iriyama, K. (1983) *Biochem.* 22: 1773-1778.
- Kuck, J.F.R. & Kuck, K.D. (1983) *Exp. Eye Res.* 36:351-362.
- Kuck, J.F.R., Yu, N.-T., & Askren, C.C. (1982) *Exp. Eye Res.* 34: 23-37.
- Ozaki, Y., Mizuno, A., Itoh, K., Yoshiura, M., Iwamoto, T., & Iriyama, K. (1983) *Biochem.* 22:6254-6259.
- Savitsky & Golay (1964) *Anal. Chem.* 36:1627.
- Spector, A. & Roy, D. (1978) *Proc. Natl. Acad. Sci.* 77:1274-1277.
- Van Haard, P.M.M., Hoenders, H.J., Wollensak, J. & Haverkamp, J. (1980) *Biochim. Biophys. Acta* 631:177-187.
- Yu, N.-T., DeNagel, D.C., Pruett, P.L., & Kuck, J.F.R. (1985) *Proc. Natl. Acad. Sci. USA* 82:7965-7968.
- Yu, N.-T., Jo, Chang, & Huber (1974) *Arch. Biochem. Biophys.* 160:614.
- Yu, N.-T. & Kuck, J.F.R. (1981) *Invest. Ophthalmol. Vis. Sci. (Suppl, ARVO abstract)* 20:132.

Figure Legends

- Figure 1. Raman spectrum of a 9 month old guinea pig lens. The Assignments for the signals are given in the text. This spectrum was taken from the geometric nuclear center of the lens.
- Figure 2. Raman spectra for a normal aging (a) and UV exposed (b) lens. UV exposure was in vivo for 9 months from time of birth. The method for measure^{ing} intensities for use in intensity ratios is demonstrated.
- Figure 3. Phenylalanine/amide I ratios (I_{622}/I_{1670}) demonstrating the linearity of the phenylalanine signal to protein concentration. For this reason, phenylalanine (622 cm^{-1}) was used as an internal standard for the disulfide signal at 508 cm^{-1} .
- Figure 4. Comparison of normal aging visual profiles of the sulfhydryl content from a 9 month (●) and 2 month old (Δ) guinea pig lens.
- Figure 5. Visual axis profiles comparing the total sulfhydryl content for a 9 month old normal lens (●) to in vivo UV irradiated lenses of 9 months (○) and 12 months (▲).
- Figure 6. Sulfhydryl visual axis profiles of contralateral lenses. One lens was exposed to 325 nm coherent radiation from a He-Cd laser for 5 hours (●); the other was analyzed as a normal aging lens (○).
- Figure 7. Disulfide profile for a normal 9 month old lens () compared to a lens exposed to in vivo long-wave UV (incoherent source) of 9 months ().



↑
Raman intensity



Wavenumber (cm^{-1})

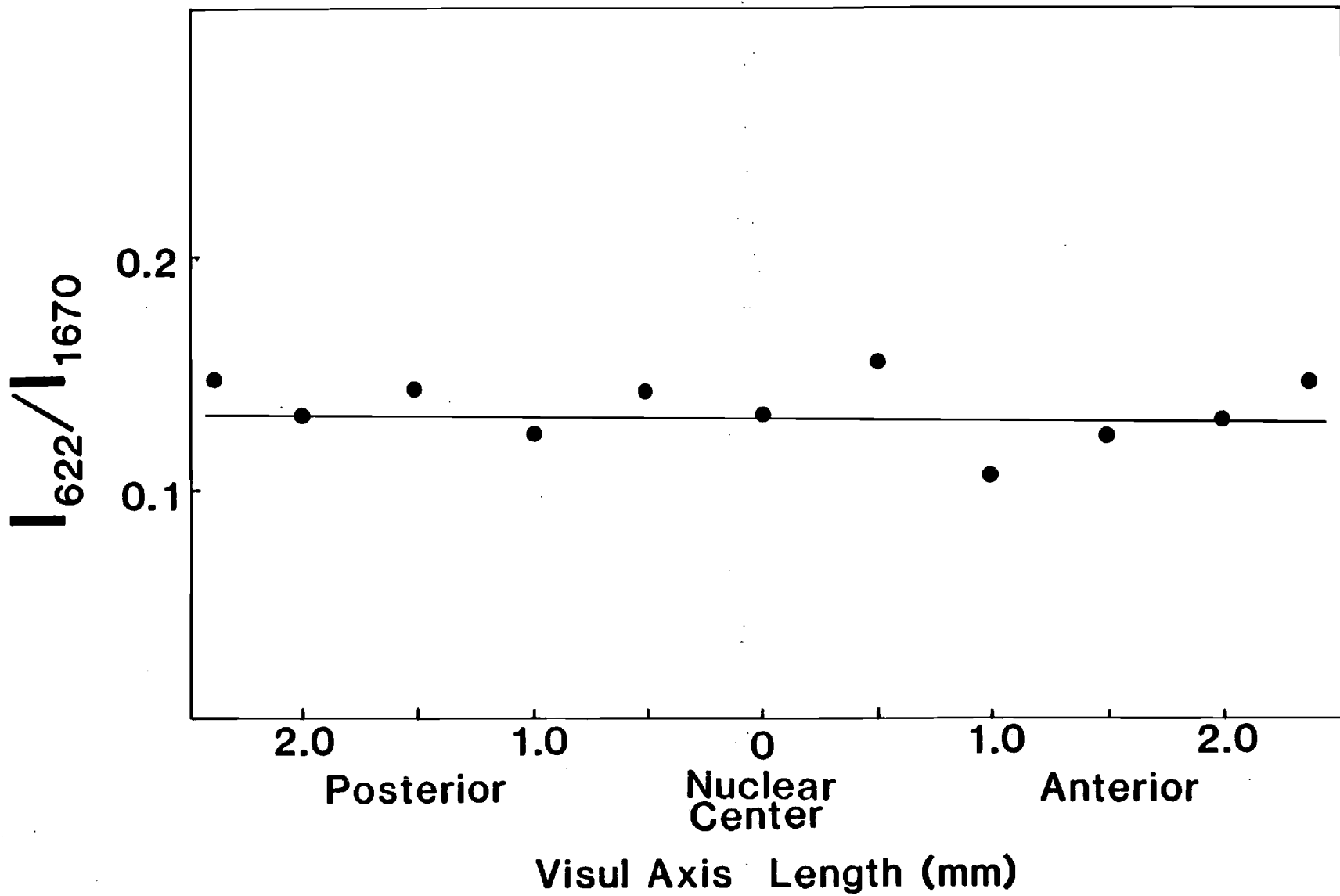


Fig 1

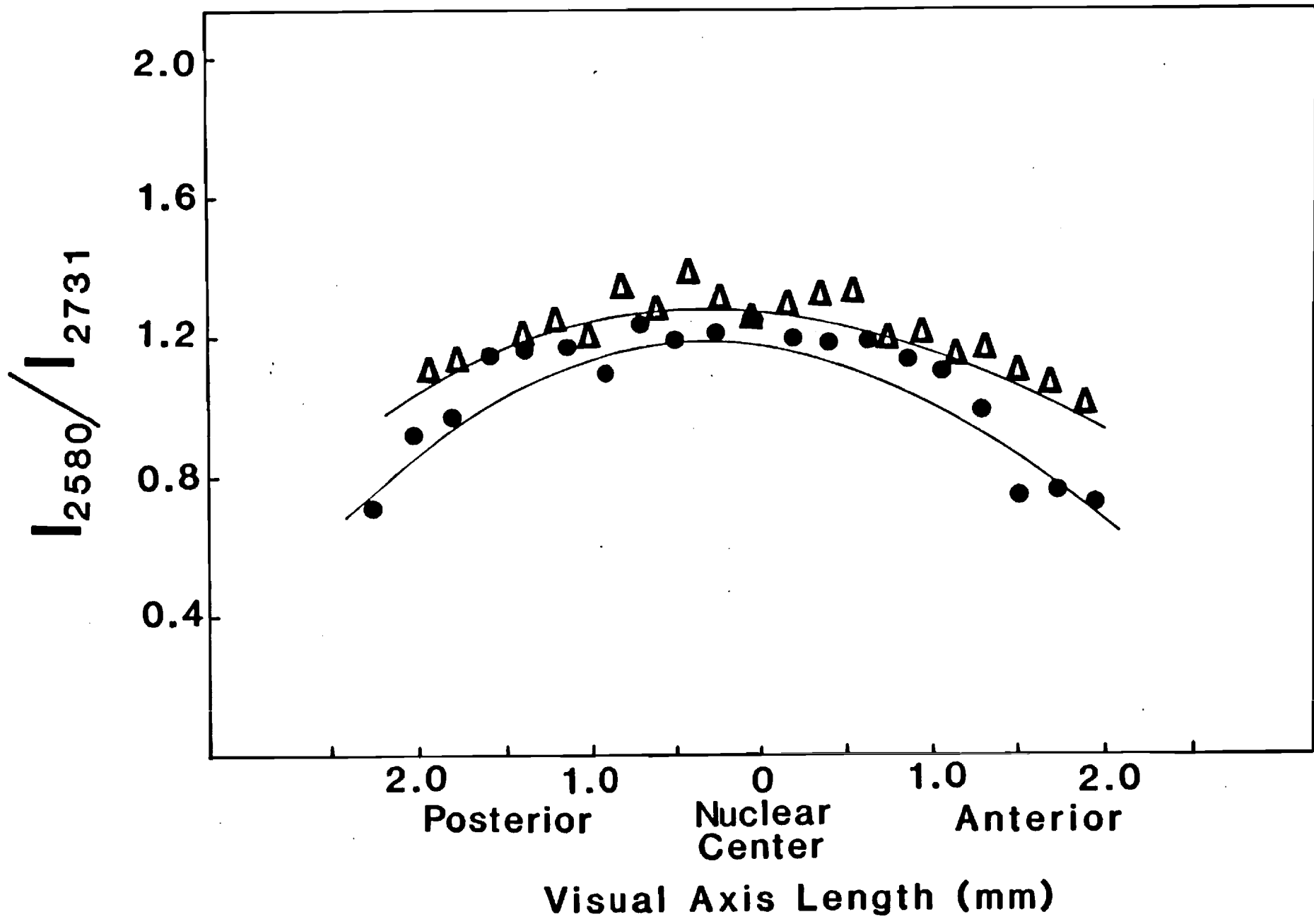


FIG 5

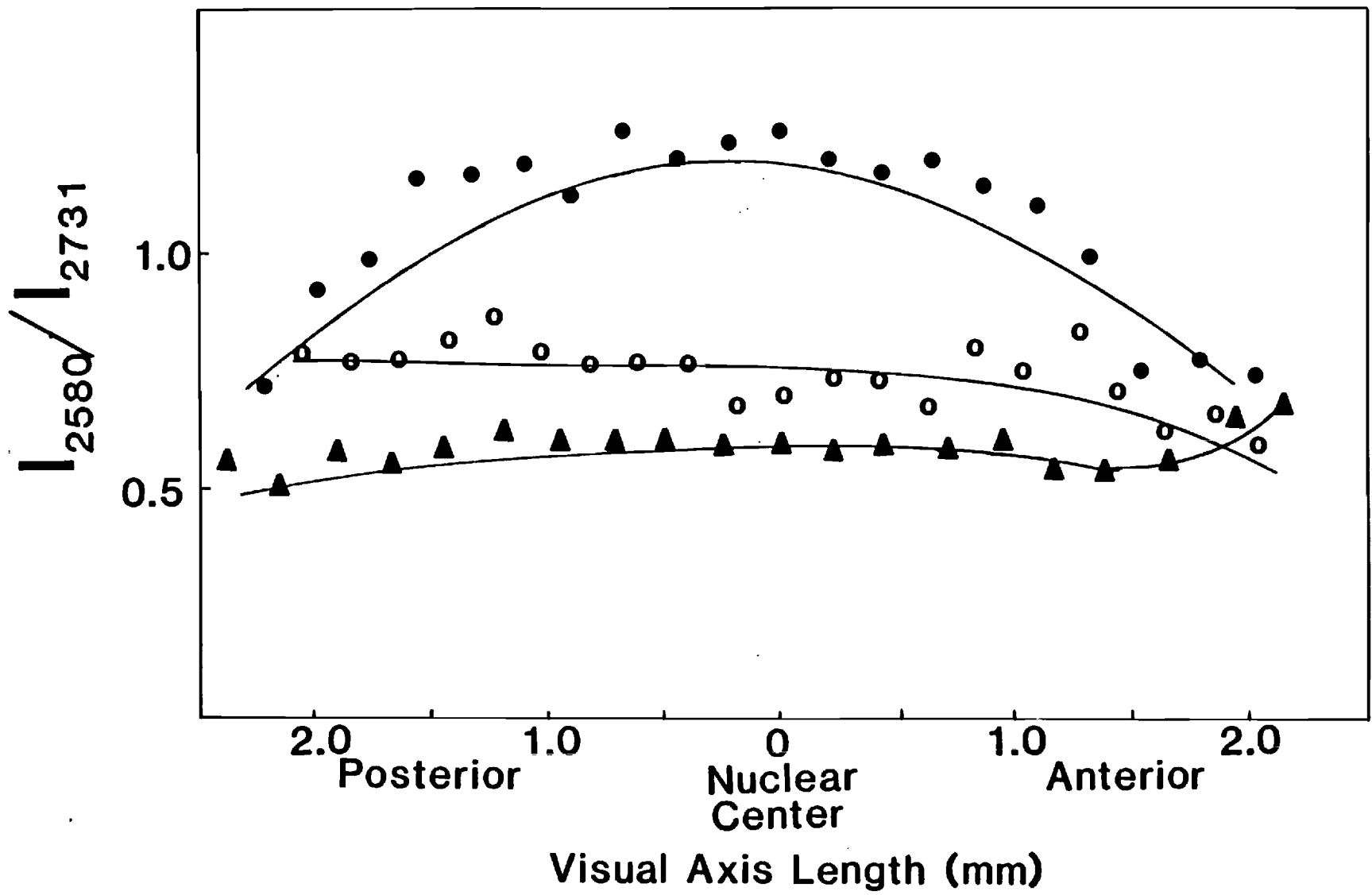


Fig 2

